

Structure of adsorbed Fe on Ni{111}

A. Theobald, V. Fernandez, O. Schaff, Ph. Hofmann, K.-M. Schindler, V. Fritzsche,
and A. M. Bradshaw

Fritz-Haber-Institut der Max-Planck-Gesellschaft, Faradayweg 4-6, 14195 Berlin-Dahlem, Germany

D. P. Woodruff

Department of Physics, University of Warwick, Coventry CV4 7AL, United Kingdom

(Received 4 March 1998)

Using photoelectron diffraction in the scanned energy mode we have established that Fe atoms adsorb in the fcc hollow sites of the Ni{111} surface even at low temperatures. Total-energy calculations had suggested that the hcp hollow sites were more stable. [S0163-1829(98)02532-6]

Because of the importance of surface and interface effects in magnetism considerable attention has focused recently on the structure of thin or ultrathin (monolayer range) iron films grown epitaxially on various metal single-crystal substrates.¹⁻¹² Such studies have recently been extended to Mn, Cr, and Co.¹³⁻²⁰ Particularly interesting, for example, has been the observation of metastable fcc, or γ -, iron phases on copper substrates up to thicknesses of a few monolayer equivalents (MLE; this is an average thickness assuming the bulk structure of the deposited material). Because the lattice parameter of γ -iron (3.59 Å, when extrapolated from above the martensitic transition at 1183 K down to room temperature) is very close to that of Cu (3.61 Å), pseudomorphic growth is expected in such systems. The structure of the first atomic layer of the film may reflect whether pseudomorphic growth occurs. In this context, Wu and Freeman²¹ have performed total-energy calculations for a monolayer of Fe on Ni{111} using the full-potential linearized-augmented-plane wave (FLAPW) method and established that the hcp hollow sites are preferred over the fcc hollow sites (the fcc Ni lattice parameter is 3.52 Å). On an fcc {111} surface the hollow sites are not identical: one distinguishes between those with an atom directly beneath in the second layer and those with an atom directly beneath in the third layer, designated ‘‘hcp’’ and ‘‘fcc,’’ respectively. In the present paper we describe photoelectron diffraction (PhD) measurements of this system using the scanned energy mode of measurement and show that even at 130 K fcc sites are predominantly occupied. Assuming the energy difference of 20 meV as calculated by Wu and Freeman,²¹ 90% occupation of hcp sites would be expected at this temperature under equilibrium conditions.

We have previously shown that photoelectron diffraction can be useful for studying the very early stages of metallic film growth.^{15,22} The technique is based on the measurement of the intensity of an adsorbate core-level photoemission peak as a function of photon energy, and thus of photoelectron kinetic energy, at a fixed emission angle.^{23,24} The observed intensity modulations are due to the interference of that component of the photoelectron wave that reaches the detector directly with those components that are first scattered from neighboring atoms. The path length differences that reflect both the direction and separation of the neighboring scatterers from the emitter atom thus contain information

on the local structure. Long-range order in the overlayer is not a necessary prerequisite, although the presence of more than two different local geometries, e.g., two different adsorption sites, does cause some problems in data analysis, unless the atoms concerned are separated by a distinct chemical shift.²⁵

The photoelectron diffraction measurements were performed on the HE-TGM-1 beamline²⁶ at the BESSY synchrotron radiation facility in Berlin. A 152-mm mean radius 150° electrostatic deflection analyzer with three parallel channeltrons (VG Scientific) was used to measure the signal at a fixed angle of 60° relative to the photon incidence direction. The Ni{111} sample was prepared by the usual combination of x-ray Laue alignment, spark machining and mechanical polishing. Argon-ion bombardment and annealing were carried out *in situ* until a clean well-ordered surface was obtained as judged by core-level photoelectron spectra and low-energy electron diffraction (LEED) pattern observations. The Fe $2p_{3/2}$ photoelectron diffraction spectra were measured at polar emission angles between 0° and 60°, in steps of 10° in four azimuths. The photoemission intensity was recorded at successive photon energies (separated by 2 eV) for kinetic energies of about ± 20 eV around the Fe $2p_{3/2}$ core-level peak to give the energy distribution curves (EDC's). The intensity of each of these peaks was then determined by background subtraction and integration. The rather broad energy interval in which we measure each EDC is necessary in order to fit the peak reliably; this is particularly necessary in the present case because of the close proximity of the Fe $2p_{1/2}$ line. The resulting intensity-energy spectra between 80 and 450 eV were normalized to give the modulation functions.

The commercially available evaporation source (Omicron) contained a piece of iron wire (purity 99.99%) heated by electron bombardment. The evaporation rate, which could be monitored by the ion current at the exit tube, was typically 0.015 MLE s⁻¹. It was calibrated by measuring the attenuation of the Ni $3p$ substrate signal as a function of time at coverages $\ll 1$ MLE. In a previous paper²² we have demonstrated that the attenuation of the substrate signal with time is a linear function of the evaporation rate a at very low coverages and is given by the equation

$$I/I_0 = 1 - (1-s)at. \quad (1)$$

$s = \exp(d/\lambda)$, where λ is the electron attenuation length in iron and at is the coverage Θ in MLE. The main source of error in the coverage determination lies in the value for λ which has to be taken from the literature. In our work on the system Cu{100}-Mn (Ref. 15) LEED patterns could be used for additional calibration. Using Eq. (1) there was agreement to within a few percent for the point at which the half-order diffraction features associated with the $(\sqrt{2} \times \sqrt{2})R45^\circ$ -Mn structure have their maximum intensity at 0.5 MLE. In general, however, the uncertainty in λ may be as high as 25%. In the present study we have used an interpolated value for λ of 14.3 Å for iron at 860 eV, as given by Tanuma, Powell, and Penn.²⁷

Quantitative structure determination of the PhD data proceeded in two stages.²⁸ The so-called projection method was first used to determine the approximate adsorption geometry, followed by a quantitative “trial-and-error” procedure in which the modulation functions are compared with the results of multiple scattering calculations.²⁹ The result of the projection method is a three-dimensional intensity map of the space around the emitter, with maximum amplitude in regions corresponding to the nearest-neighbor backscatterers. It therefore gives the adsorption site and an approximate value for the adsorbate-substrate separation. The calculations in the second stage are performed on the basis of an expansion of the final-state wave function into a summation over all scattering pathways that the electron can take from the emitter atom to the detector outside the sample. A magnetic quantum number expansion is used to calculate the scattering contribution of an individual scattering path.²⁹ The finite energy resolution and angular acceptance of the electron energy analyzer are explicitly included. Anisotropic vibrations for the emitter atom and isotropic vibrations for the scattering atoms are also taken into account. The comparison between theory and experiment is aided by the use of a reliability factor

$$R_m = \sum (\chi_{th} - \chi_{ex})^2 / \sum (\chi_{th}^2 + \chi_{ex}^2), \quad (2)$$

for which a value of 0 corresponds to perfect agreement, a value of 1 to completely uncorrelated data, and a value of 2 to completely anticorrelated data.²⁸ The uncertainties in the optimized parameters can be estimated by following the guidelines suggested by Pendry³⁰ for the analysis of LEED I - V data.³¹

The quantitative PhD analysis was carried out at a coverage of 0.6 MLE. Figure 1 shows modulation functions measured at 130 K for eight different emission angles after deposition at 200 K (bold lines); the modulation functions for the same coverage obtained after deposition at 130 K were virtually identical. The strong, single oscillations at certain angles suggest that these emission directions are dominated by 180° , or near 180° , backscattering from nearest-neighbor substrate atoms. This is confirmed by the results of the projection method shown in Fig. 2. The gray-scale plots represent sections through a three-dimensional map in a volume of real space “below” the emitter. Dark areas correspond to high values of the projection coefficient $C(x,y,z)$ and indicate the location of a nearest-neighbor backscatterer. Figure

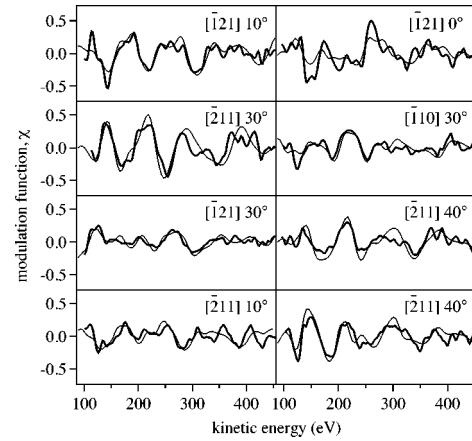


FIG. 1. Bold curves: Fe $2p_{3/2}$ modulation functions in eight different directions for a 0.6 MLE iron layer deposited on a Ni{111} surface at 200 K. Temperature of the measurement = 130 K. Faint curves: multiple scattering simulations for an iron monolayer.

2 shows a cut perpendicular to the surface in the $[\bar{2}11]$ direction indicating a maximum in $C(x,y,z)$ about 2 Å below the emitter (Fe) atom. The corresponding section parallel to the surface, i.e., in the xy plane, at $z = -2.0$ Å shows that there are actually three such features. This configuration of nearest-neighbor backscatterers immediately indicates that the Fe atom is situated in a threefold symmetric hollow site. Moreover, because of the azimuthal orientation of the pattern relative to the known crystal directions, it is readily apparent that it is the fcc hollow site that is occupied. Having established the “adsorption site,” the full trial-and-error analysis was carried out for three different model structures, namely,

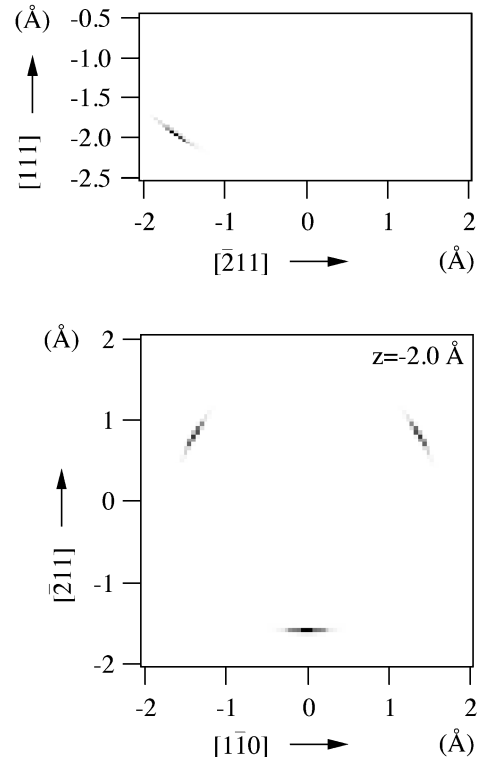


FIG. 2. Results from the application of the projection method to the Ni{111}-Fe system at 0.6 MLE.

TABLE I. Resulting parameters for the three model structures.

Parameter	Monolayer	Bilayer	Ni-Fe-Ni sandwich
d_{12}	2.00(3)	2.00(4)	2.00(3)
d_{13}	4.04(4)	4.04(4)	4.03(8)
d_{14}	6.16(16)	5.99(11)	6.06(36)

a simple Fe monolayer, an Fe monolayer covered with a Ni monolayer (i.e., a “sandwich” structure to account for possible segregation effects), and an Fe bilayer. The parameters varied were d_{12} , the separation between the first and second layers of the model structure, d_{13} , the first to third layer separation, and d_{14} , the first to fourth layer separation. The R factors obtained were 0.22, 0.27, and 0.26, respectively, for the three model structures. The best-fit calculated modulation functions for the monolayer are shown in Fig. 1 (thin lines). Although the theoretical curves reproduce well all the main structure of the experimental curves, the latter do appear to show some fine structure above the noise level that is not well matched. It is possible that this indicates that the role of more distant scatterers (longer scattering paths) is slightly more important than is reflected by the calculation. The structural parameters for the three models are given in Table I. We note that the Fe-Ni layer separation in the monolayer is 2.00 Å, compared to 1.92 Å in the calculation of Wu and Freeman²¹ for the fcc site.

Although the monolayer is the most likely structure, the variance (0.04) is such that the bilayer cannot be excluded. Indeed, a mixture of monolayer and bilayer is also possible, but an optimization of the relative proportions does not give a significant result since the R factors are very similar and the structural parameters d_{12} and d_{13} are identical. In order to see whether a certain percentage of hcp sites could also be present (the logarithmic intensity scale of the projection method maps tends to suppress the contribution from “mi-

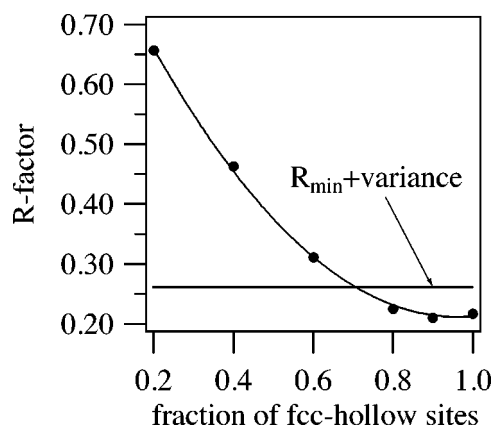


FIG. 3. R factor as a function of the fractional fcc/hcp site occupation for the system Ni{111}-Fe at 0.6 MLE.

nority” species), the fcc/hcp ratio has also been optimized for the monolayer. The results are shown in Fig. 3 in which a parabola has been fitted to the calculated R factors. The minimum in the R factor occurs for a 100% fcc layer, but the variance is such that up to 25% hcp sites might be present. For present purposes, however, the most important conclusion is that the fcc site is strongly favored. As noted above, the calculations of Wu and Freeman²¹ had indicated that the hcp site was marginally more stable, which might have led to the growth of an hcp phase.

The authors are pleased to acknowledge financial support of this work in the form of grants from the Deutsche Forschungsgemeinschaft through the Sonderforschungsbereich 290, the Federal Ministry for Education, Science, Research and Technology (Germany) under Contract No. 05 625 EBA 6, the Engineering and Physical Sciences Research Council (U.K.) and the European Union through a Human Capital and Mobility network (No. ERBCHRX CT930358) and the Large-Scale Facilities Programme.

¹Y. Darici, J. Marcano, H. Min, and P. A. Montano, Surf. Sci. **195**, 566 (1988).

²D. Tian, F. Jona, and P. M. Marcus, Phys. Rev. B **45**, 11 216 (1992).

³M. T. Kief and W. F. Egelhoff, Jr., J. Vac. Sci. Technol. A **11**, 1661 (1993).

⁴A. Brodde, K. Dreps, J. Binder, Ch. Lunau, and H. Neddermeyer, Phys. Rev. B **47**, 6609 (1993).

⁵K. Heinz, S. Müller, and P. Bayer, Surf. Sci. **337**, 215 (1995).

⁶S. H. Hu, J. Quinn, D. Tian, F. Jona, and P. M. Marcus, Surf. Sci. **209**, 364 (1989).

⁷S. Müller, P. Bayer, C. Reischl, K. Heinz, B. Feldmann, H. Zillgen, and M. Wuttig, Phys. Rev. Lett. **74**, 765 (1995).

⁸S. H. Lu, Z. Q. Wang, D. Tian, Y. S. Li, F. Jona, and P. M. Marcus, Surf. Sci. **221**, 35 (1991).

⁹C. Liu and S. D. Bader, J. Vac. Sci. Technol. A **8**, 2727 (1990).

¹⁰H. Bethge, D. Heuer, Ch. Jensen, K. Reshöft, and U. Köhler, Surf. Sci. **331–333**, 878 (1995).

¹¹G. W. Anderson and P. R. Norton, Surf. Sci. **336**, 262 (1995).

¹²H. J. Elmers and J. Hauschild, Surf. Sci. **320**, 134 (1994).

¹³M. Wuttig, Y. Gauthier, and S. Blügel, Phys. Rev. Lett. **70**, 3619 (1993).

¹⁴H. P. Noh, T. Hashizume, D. Jeon, Y. Kuk, H. W. Pickering, and T. Sakurai, Phys. Rev. B **50**, 2735 (1994).

¹⁵R. Toomes, A. Theobald, R. Lindsay, T. Gießel, O. Schaff, R. Didzuhn, D. P. Woodruff, A. M. Bradshaw, and V. Fritzsche, J. Phys.: Condens. Matter **8**, 10 231 (1996).

¹⁶M. T. Kief and W. F. Egelhoff, Jr., Phys. Rev. B **47**, 10 785 (1993).

¹⁷S. Müller, G. Kostka, T. Schäfer, J. de la Figuera, J. E. Prieto, C. Ocal, R. Miranda, K. Heinz, and K. Müller, Surf. Sci. **352–354**, 46 (1996).

¹⁸S. K. Kim, F. Jona, and P. M. Marcus, Surf. Sci. **349**, 160 (1996).

¹⁹M. E. Haugan, Qibiao Chen, M. Onellion, and F. J. Himpsel, Phys. Rev. B **49**, 14 028 (1994).

²⁰D. Rouyer, C. Krembel, M. C. Hanf, D. Blomont, and G. Gewinner, Surf. Sci. **331–333**, 957 (1995).

²¹R. Wu and A. J. Freeman, Phys. Rev. B **45**, 7205 (1992).

²²A. Theobald, S. Bao, V. Fernandez, K.-M. Schindler, O. Schaff, V. Fritzsche, A. M. Bradshaw, N. Booth, and D. P. Woodruff, Surf. Sci. **385**, 107 (1997).

- ²³D. P. Woodruff and A. M. Bradshaw, Rep. Prog. Phys. **57**, 1029 (1994).
- ²⁴A. M. Bradshaw and D. P. Woodruff, in *Applications of Synchrotron Radiation*, edited by W. Eberhardt, Springer Series in Surface Science, Vol. 35 (Springer-Verlag, Berlin, 1995).
- ²⁵K.-U. Weiss, R. Dippel, K.-M. Schindler, P. Gardner, V. Fritzsche, A. M. Bradshaw, D. P. Woodruff, M. C. Asensio, and A. R. Gonzalez-Elipe, Phys. Rev. Lett. **71**, 581 (1993).
- ²⁶E. Dietz, W. Braun, A. M. Bradshaw, and R. L. Johnson, Nucl. Instrum. Methods Phys. Res. A **239**, 359 (1985).
- ²⁷S. Tanuma, C. J. Powell, and D. R. Penn, Surf. Interface Anal. **17**, 991 (1991).
- ²⁸Ph. Hofmann, K.-M. Schindler, S. Bao, V. Fritzsche, A. M. Bradshaw, and D. P. Woodruff, Surf. Sci. **337**, 169 (1995).
- ²⁹V. Fritzsche, Surf. Sci. **265**, 187 (1992), and references therein.
- ³⁰J. B. Pendry, J. Phys. C **13**, 937 (1980).
- ³¹N. A. Booth, R. Davis, R. Toomes, D. P. Woodruff, C. Hirschmugl, K. M. Schindler, O. Schaff, V. Fernandez, A. Theobald, Ph. Hofmann, R. Lindsay, T. Gießel, P. Baumgärtel, and A. M. Bradshaw, Surf. Sci. **387**, 152 (1997).